THE JOURNAL OF BIOLOGICAL CHEMISTRY
Vol. 279, No. 21, Issue of May 21, pp. 21833–21840, 2004

Printed in U.S.A.

A Designed Probe for Acidic Phospholipids Reveals the Unique Enriched Anionic Character of the Cytosolic Face of the Mammalian Plasma Membrane*

Received for publication, December 9, 2003, and in revised form, March 4, 2004
Published, JBC Papers in Press, March 8, 2004, DOI 10.1074/jbc.M313469200

Nicole M. Okeley and Michael H. Gelb‡

From the Departments of Chemistry and Biochemistry, University of Washington, Seattle, Washington 98195

It is generally accepted that the cytosolic face of the plasma membrane of mammalian cells is enriched in acidic phospholipids due to an asymmetric distribution of neutral and anionic phospholipids in the two bilayer leaflets. However, the phospholipid asymmetry across intracellular membranes is not known. Two models have been proposed for the selective targeting of K-Ras4B, which contains a C-terminal farnesyl cysteine methyl ester adjacent to a polybasic peptide segment, to the cytosolic face of the plasma membrane. One involves electrostatic interaction of the lipidated polybasic domain with anionic phospholipids in the plasma membrane, and the other involves binding of K-Ras4B to a specific protein receptor. To address this issue, we prepared by semi-synthesis a green fluorescent protein variant that is linked to a farnesylated, polybasic peptide corresponding to the K-Ras4B C terminus as well as a variant that contains an *all*-D amino acid version of the K-Ras4B peptide. As expected based on electrostatics, both constructs showed preferential *in vitro* binding to anionic phospholipid vesicles *versus* those composed only of zwitterionic phospholipid. Both constructs fully targeted to the plasma membrane when microinjected into live Chinese hamster ovary and Madin-Darby canine kidney cells. Because the *all*-D amino acid peptide should be devoid of binding affinity to a putative highly specific K-Ras membrane receptor, these results support an electrostatic basis for the targeting of K-Ras4B to the plasma membrane, and they support an intracellular landscape of phospholipids in which the cytosolic face of the plasma membrane is the most enriched in acidic phospholipids.

It is well known that the lipids that constitute the plasma membrane of eukaryotic cells are asymmetrically distributed across the two bilayer leaflets (1, 2). Using techniques that include selective degradation of extracellular facing phospholipids and covalent modification of lipids by cell impermeable agents (2, 3), it was established that the outer leaflet of the plasma membrane contains most of the phosphatidylcholine (PC)[1] and sphingomyelin, whereas the intracellular leaflet is enriched in phosphatidylethanolamine and the anionic phospholipids phosphatidylserine (PS) and phosphatidylinositol. Such techniques are applicable to the study of the plasma membrane, however, experimental approaches to explore the lipid asymmetry of intracellular membranes are lacking. Phospholipid asymmetry of the plasma membrane is maintained by energy-dependent phospholipid translocases (4–6), and phospholipid transfer between plasma and intracellular membranes may intuitively suggest that internal membranes should have the same phospholipid asymmetry as the plasma membrane, with PS of internal membranes facing the cytosol rather than the lumen of the Golgi and endoplasmic reticulum (ER). However, current evidence favors energy-independent, protein-mediated equilibration of all classes of phospholipids across the ER membrane (7), which is needed to move biosynthesized phospholipids from their site of membrane insertion on the cytosolic face of ER membranes to the luminal face. If these phospholipid translocation events are fast on the time scale of intermembrane phospholipid transfer, distinct patterns of phospholipid asymmetry in different cellular membranes may exist. To date, there is no data that clearly establishes the distribution of phospholipids across the two leaflets of eukaryotic cell internal membranes.

Selective targeting of peripheral membrane proteins to specific cellular membranes suggests that the cytosolic face of the plasma membrane is selectively enriched in anionic phospholipids, whereas the cytosolic face of intracellular membranes lacks such asymmetry. For example, cytosolic phospholipase A_2 ($cPLA_2$) is targeted to the perinuclear region of cells, including the nuclear envelope, ER, and Golgi (8, 9), and prefers PC-rich over PS-rich membranes *in vitro* (10, 11). Other proteins display preferential *in vitro* binding to PS-rich membranes compared with those rich in PC and are known to localize to the cytosolic face of the plasma membrane, for example K-Ras4B (12, 13) and Src kinase (14–16), which contain lipid anchors adjacent to a string of lysine and arginine residues. It has been suggested that the electrostatic interaction of a polybasic domain with acidic phospholipids is the basis of K-Ras4B and SRC binding to the plasma membrane. The C terminus of the K-Ras4B protein, consisting of the sequence GKKKKKKSKT-KC(*S*-farnesyl)-COOMe, binds several orders of magnitude more tightly to PC vesicles that contain PS *versus* vesicles that

* This work was supported by National Institutes of Health (NIH) Grant HL50040 (to M. H. G.) and an NIH Postdoctoral Fellowship HL71405 (to N. M. O.). The costs of publication of this article were defrayed in part by the payment of page charges. This article must therefore be hereby marked "*advertisement*" in accordance with 18 U.S.C. Section 1734 solely to indicate this fact.

‡ To whom correspondence should be addressed. Tel.: 206-543-7142; Fax: 206-685-8665; E-mail:gelb@chem.washington.edu.

[1] The abbreviations used are: PC, phosphatidylcholine; CHO, Chinese hamster ovary; $cPLA_2$, cytosolic phospholipase A_2-α; ESI, electrospray ionization; GFP, green fluorescent protein; EGFP, enhanced GFP; sgGFP, SuperGlo™ GFP; MALDI, matrix-assisted laser desorption ionization; MDCK, Madin-Darby canine kidney; POPC, 1-palmitoyl-2-oleoyl-*sn*-glycero-3-phosphocholine; POPS, 1-palmitoyl-2-oleoyl-*sn*-glycero-3-(phospho-L-serine); PS, phosphatidylserine; RP-HPLC, reversed phase-high performance liquid chromatography; ER, endoplasmic reticulum; LUV, large unilamellar vesicle; BisTris, 2-[bis(2-hydroxyethyl)amino]-2-(hydroxymethyl)propane-1,3-diol; DTT, dithiothreitol; MOPS, 4-morpholinepropanesulfonic acid; NLS, nuclear localization signal.

lack the acidic phospholipid (13, 17). *In vivo* experiments have shown that sequential mutation of the lysines to glutamines causes a progressive reduction in the amount of K-Ras4B bound to the cytosolic side of the plasma membrane, whereas mutation of all of the lysines to arginine residues does not affect plasma membrane targeting (18). Similar results have been observed with the SRC N-terminal domain (19, 20), which contains an N-terminal myristoyl group followed by a peptide segment enriched in basic residues.

Despite this support for a major electrostatic role in K-Ras4B and SRC targeting, the mechanism by which these proteins are targeted to the cytosolic face of the plasma membrane is still debated. Membrane targeting may be due to other proteins, perhaps integral membrane proteins, which function as a targeting scaffold or constitute a member of a signaling network that forms on the membrane surface. Analogs of *S*-farnesylcysteine have recently been shown to displace K-Ras4B from the plasma membrane (21), suggesting that the analog is competing with K-Ras4B for binding to a specific membrane target. Additionally, microtubules may act to deliver the fully matured K-Ras4B protein, based on the observation that disruption of the microtubular network prevents proper localization of K-Ras4B at the plasma membrane in NIH3T3 cells (22–24). A putative receptor for SRC has also been detected in cell extracts (25), and the intermediate filament protein vimentin has been proposed to function as a targeting protein for $cPLA_2$ (26). It is apparent that a probe for the acidic phospholipid-rich membrane compartments is needed and that such a probe should lack structural features that would be expected to undergo specific interactions with putative, membrane-bound targeting receptors. In the present study, we have developed such a probe based on the C terminus of K-Ras4B and have studied its targeting in mammalian cells.

MATERIALS AND METHODS

Mass spectrometry was performed using electrospray ionization (ESI) or matrix-assisted laser desorption ionization (MALDI). Reversed phase-high performance liquid chromatography (RP-HPLC) was carried out with Vydac 218TP columns (preparative 2.2 × 25 cm, semi-preparative 1 × 25 cm), developed with solvent A (0.06% trifluoroacetic acid, in water) and solvent B (0.06% trifluoroacetic acid in MeCN) using program 1, 0% B for 15 min, 0–50% B in 30 min, and then 80–100% B in 20 min, or program 2, 0–30% B for 5 min, 30–50% B in 30 min, and then 80–100% B in 20 min, and detection at 220 nm.

Peptide Modifications—Crude, resin-bound peptides were synthesized by SynPep Corp. on chlorotrityl resin (0.15-mmol scale). The peptides possessed free N termini and Fmoc (*N*-(9-fluorenyl)methoxycarbonyl)-compatible protected side chains. N-terminal acetylation was accomplished by addition of acetic anhydride (2 ml) to the resin swollen in 6 ml of 0.4 M *N*-methylmorpholine in dimethyl formamide with stirring for 1.5 h. The beads were washed with *N*-methylpyrrolidone (3 × 5 ml) and CH_2Cl_2 (2 × 5 ml).

Peptides were released from the resin with 10 ml of 1% trifluoroacetic acid in CH_2Cl_2 for 15 min with stirring. Beads were washed with CH_2Cl_2 (3 × 6 ml) and trifluoroethanol (2 × 5 ml), and the cleavage procedure was repeated twice. The combined filtrates were concentrated to a pale yellow solution, which was diluted with CH_2Cl_2 and re-concentrated. This was repeated until almost no color lingered and a foamy solid remained.

The crude *all*-L peptide (1.122 g) was dissolved in 110 ml of CH_2Cl_2 containing 0.5 ml of trifluoroethanol. A solution of diazomethane in ether (from Diazald, Aldrich) was added dropwise until a yellow color persisted. After 30 min at room temperature, a few drops of dilute acetic acid were added. The solvent was removed, producing a foamy solid (0.781 g).

Side-chain protecting groups were cleaved from the *all*-L peptide methyl ester by stirring for 10 min with 16 ml of 93% trifluoroacetic acid, 5% thioanisole, 1% water, 0.5% phenol, followed by portion-wise addition of triisopropylsilane (82 μl, ~1.4 eq based on crude mass) in trifluoroacetic acid (2 ml) over 2 h. The trifluoroacetic acid solution was added dropwise to 60 ml of ice-cold ether. The suspension was shaken and placed on ice for 10 min, followed by centrifugation at 5900 × *g* at 4 °C for 20 min. The pellet was washed with 10 ml of ice-cold ether and dried under water aspiration for 15 min. The peptide was dissolved in 3 ml of 2:1 1% acetic acid:MeCN and was purified by RP-HPLC (0.224 g, retention time 40.1 min, semi-preparative column, 1.5 ml/min, program 1). ESI-MS *m/z* calcd. for $((M+3)/3)^+$ 547.0, $((M+2)/2)^+$ 820.0, found 547.6, 820.4.

The deprotected *all*-L peptide (0.100 g) was farnesylated as previously described (13, 27), except the reaction was allowed to proceed overnight (16 h). Farnesylated peptide was isolated by RP-HPLC (0.0312 g, retention time 48.8 min, semi-preparative column, 1.5 ml/min, program 1). ESI-MS *m/z* calcd. for $((M+3)/3)^+$ 615.0, $((M+2)/2)^+$ 922.1, found 615.6, 922.7.

The farnesylated *all*-L peptide (11.9 mg) was dissolved in 1.11 ml of 3.4:1 water:MeCN and diluted with 3.32 ml of 50 mM NH_4OAc, pH 7.6. A fresh solution of Tris(2-carboxyethyl)phosphine (150 mM, 430 μl) in 20 mM HEPES, pH 7.0, was added. The flask was flushed with argon, and the reaction was stirred at room temperature overnight (16 h). The product was isolated by RP-HPLC (8.6 mg, retention time 50.3 min, semi-preparative column, 1.5 ml/min, program 1). ESI-MS *m/z* calcd. for $((M+3)/3)^+$ 585.7, $((M+2)/2)^+$ 878.1, found 586.2, 878.3. The acetylated and farnesylated *all*-D peptide methyl ester was prepared in the same manner as the *all*-L peptide.

Peptide-Linker Synthesis—Iodoacetic acid (158 mg) was dissolved in dry CH_2Cl_2 (5.15 ml) under nitrogen. The flask was wrapped in aluminum foil and cooled in an ice water bath. Dicyclohexylcarbodiimide (143 mg) was added in one portion. The solution was stirred for 1 h on ice, and a solution of 4,7,10-trioxa-1,13-tridecanediamine (80 μl, Fluka) in dry tetrahydrofuran (0.85 ml) was added via syringe. The reaction was stirred, the ice was allowed to melt over 4 h, and stirring was continued overnight. A white precipitate was removed by filtration, and the filtrate was concentrated to a pale yellow film. More solid was precipitated by adding ethyl acetate (EtOAc) and CH_2Cl_2 (1:1, 10 ml). The suspension was filtered and concentrated. The film was dissolved in CH_2Cl_2 and loaded onto a silica column developed with CH_2Cl_2 and EtOAc, followed by MeCN (R_F = 0.34 in 100% MeCN) to give 142 mg of linker. ^{1}H NMR (200 MHz, $CDCl_3$): δ ppm 1.7 (quintet, 4H, J = 6.3 Hz), 3.3 (q, 4H, J = 6.0 Hz), 3.5–3.6 (m, 12H), 3.6 (s, 4H), 6.8 (br s, 1H, N*H*); ESI-MS *m/z* calcd. for $(M+1)^+$ 557.0, found 556.8.

Linker (4.8 mg) was dissolved in dimethyl formamide (14.7 μl) and was diluted in 50 mM HEPES, pH 8.0 (1.96 ml). An aqueous solution of farnesylated *all*-L peptide (0.86 mg in 10 μl) was added. The flask was flushed with nitrogen, sealed, and wrapped in aluminum foil, and the reaction was stirred at room temperature for 2 h. The product was purified by RP-HPLC (0.4 mg, retention time 31.2 min, preparative column, 5 ml/min, program 2). ESI-MS *m/z* calcd. for $((M+3)/3)^+$ 728.4, $((M+2)/2)^+$ 1092.1, found 728.9, 1093.3.

Protein Purification—pQBIT7-GFP, encoding sgGFP (SuperGlo™ green fluorescent protein, QBiogene), was subjected to site-directed mutagenesis using the QuikChange® method of Stratagene. The mutation was verified by DNA sequencing. sgGFP N239C was overexpressed in *Escherichia coli* strain BL21(DE3) by induction with 0.5 mM isopropyl-β-D-thiogalactopyranoside in LB medium with ampicillin with shaking at room temperature for 3 h. Cells were harvested by centrifugation. The purification procedure was that of Alakhov and coworkers (28), except protein was released from the cells by subjection to three cycles of freezing and thawing (29). Purified protein was exchanged into buffer A (20 mM BisTris, pH 6.4) by dilution and concentration using a Diaflo® PM10 ultrafiltration membrane (Amicon). The concentrated protein was treated with 5 mM DTT and stored at −20 °C. MALDI-MS *m/z* calcd. $(M\text{-}Met+H)^+$ 26,800, found 26,790.

Peptide-Protein Conjugation—Immediately prior to conjugation, sgGFP N239C was further purified on a Q-Sepharose HP FPLC column (0.5 ml, Amersham Biosciences) at 4 °C to remove the DTT and residual protein disulfide dimer. After sample injection the column was washed with buffer A (10 min, 0.25 ml/min) and eluted with a gradient of 0–0.25 M NaCl in buffer A over 42 min. Monomeric sgGFP N239C (retention time 41.4 min) was exchanged into 50 mM HEPES, 5 mM EDTA, pH 8.0, by passing through a Sephadex G-25 gel filtration column (70 ml). sgGFP N239C was concentrated by Centriprep-10 (Amicon) at 4 °C. Protein concentration was estimated using the extinction coefficient at 280 nm based on amino acid composition (ε 20,010 M^{-1} cm^{-1}).

A 7× stock solution of the Complete Mini Protease Inhibitor Mixture from Roche Applied Science (141.6 μl) was added to the sgGFP N239C (805 μl, 0.69 mg/ml). One equivalent of peptide-linker in water (4 μg/μl, 11.2 μl) was added, and the reaction was placed on ice. Approximately every 30 min another equivalent of peptide-linker was added until the fourth equivalent, after which the reaction was kept on ice for an

additional 2 h and was stored at −20 °C overnight.

After thawing on ice, the reaction was treated with DTT (10 mM) for 10 min and was loaded onto a freshly packed 0.5-ml Q-Sepharose HP FPLC column. The column was washed with buffer A (21 min, 0.25 ml/min) and was eluted with a linear gradient of 0–0.25 M NaCl in buffer A over 42 min. Fractions (0.25 ml) were analyzed by 15% SDS-PAGE, and those containing conjugate (retention time 38.3 min) were combined and concentrated by Microcon-10 (Amicon) at 4 °C. MALDI-MS m/z calcd. $(M+H)^+$ 28,854, found 28,939.

Vesicle Binding Studies—Solutions of phospholipids in $CHCl_3$ (1-palmitoyl-2-oleoyl-*sn*-glycero-3-phosphocholine, POPC, and 1-palmitoyl-2-oleoyl-*sn*-glycero-3-(phospho-L-serine), POPS, Avanti Polar Lipids) were mixed together in a glass tube, along with a small amount of radiolabeled phospholipid as tracer (L-α-dipalmitoyl [2-palmitoyl-9,10-^{3}H]phosphatidylcholine or L-α-dipalmitoyl [dipalmitoyl-1-^{14}C]phosphatidylcholine (American Radiolabeled Chemicals, Inc.). Solvent was removed with a nitrogen stream, and the tubes were then placed *in vacuo* for 30 min. Large unilamellar vesicles (LUVs) of 30 mM POPS/POPC (20%/80%, doped with ^{3}H tracer), 125 mM POPS/POPC (20%/80%, doped with ^{14}C tracer), or 200 mM POPC (doped with ^{14}C tracer) were prepared by suspending the lipid film in buffer, briefly vortexing, and subjecting the sample to 8 freeze/thaw/vortex cycles (vortex 30 s). Suspensions were passed 21 times through a LiposoFast syringe device (Avestin) containing two 800-nm filters and then 21 times through two 100-nm filters (Whatman).

POPC vesicles and 125 mM POPS/POPC vesicles were extruded in 5 mM MOPS, pH 7.4, 0.1 M KCl, and 30 mM POPS/POPC vesicles in 5 mM MOPS, pH 7.4, 176 mM sucrose. Extruded solutions were diluted 4-fold in buffer B (5 mM MOPS, pH 7.4, 182 mM glucose) and centrifuged at 99,200 × g at 21 °C for 1 h. For the KCl-loaded POPC and POPS/POPC vesicles, the supernatant was removed and utilized for binding studies, whereas for the sucrose-loaded POPS/POPC vesicles, the pellet was resuspended in buffer B and used for binding studies. Lipid concentration after centrifugation was determined by scintillation counting.

Sucrose-loaded POPS/POPC LUVs and buffer B were added to 10 polyallomer microcentrifuge tubes to give 2 mM lipid in 100 μl. Approximately 25 pmol of sgGFP-L-tK was added to tubes 1–5, and 18 pmol of sgGFP-D-tK was added to tubes 6–10. Tubes were tapped gently to mix and centrifuged at 99,200 × g, 21 °C for 45 min. Supernatant (95 μl) was carefully removed, and pellets were resuspended with the following amounts of POPC vesicles in buffer B (95 μl): tubes 1 and 6, 0 mM; tubes 2 and 7, 2 mM; tubes 3 and 8, 4 mM; tubes 4 and 9, 10 mM; and tubes 5 and 10, 20 mM. Tubes were centrifuged at 99,200 × g, 21 °C for 45 min, were immediately frozen in a dry ice-acetone bath, and cut with a razor blade 4 mm from the bottom, and the two frozen halves were diluted to 1 ml with 5 mM MOPS, pH 7.4, 0.1 M KCl, 1.8 mg/ml deoxycholate. The fluorescence was measured on a fluorometer with excitation at 474 nm and emission at 509 nm. Subsequently, 0.9 ml of each sample was submitted to scintillation counting, and the amount of ^{3}H and ^{14}C was determined by double-channel analysis. A control experiment using the KCl-loaded POPS/POPC vesicles as the chase vesicles was also performed. The procedure was as described for the POPC chase vesicles.

Cell Culture and Transfection—pEGFP-C2cPLA$_2$, encoding enhanced green fluorescent protein (EGFP) fused to the C2 domain of cPLA$_2$, was provided by C. Leslie (National Jewish Medical and Research Center), and pEGFP-tK and pEGFP-K-Ras, encoding an EGFP fusion with the K-Ras4B C-terminal 17 residues and full-length K-Ras4B, respectively, were provided by J. Hancock (30). Madin-Darby canine kidney cells (MDCK, ATCC) were grown in Eagle's modified minimum essential medium (ATCC #30-2003) supplemented with 10% fetal bovine serum in a humidified environment of 5% CO_2 at 37 °C. Chinese hamster ovary cells (CHO, ATCC) were grown in Ham's nutrient mixture F-12 (Sigma #N6658) supplemented with 10% fetal bovine serum.

Plasmids were prepared from bacterial cultures using the SNAP™ midiprep kit (Stratagene). Transfections of CHO cells were carried out by the LipofectAMINE™ method (Invitrogen). Stable transfectants were selected by limiting dilution in medium containing 0.6 mg/ml Geneticin (Invitrogen). Colonies were examined by fluorescence microscopy for expression of the EGFP fusion proteins. Transfection for paclitaxel studies was performed as described by Chen *et al.* (22) using either pEGFP-tK or pEGFP-K-Ras.

Preparation of C2-cPLA$_2$ Alexa Fluor®-488 Conjugate—The K113C mutant C2-domain of cPLA$_2$ was prepared as described previously (31) and was reacted with the fluorescent marker Alexa Fluor® 488 C_5 maleimide (Molecular Probes). The protein solution (25–100 μM) in 50 mM HEPES, pH 7.0, was treated with 7.5 eq of Tris(2-carboxyethyl)phosphine at room temperature for 1 h, followed by treatment with 7.5 eq of probe-maleimide for 2 h. Free fluorophore was removed by repeated dilution/concentration cycles.

Microinjection and Confocal Microscopy—Microinjection was with a Leitz mechanical micromanipulator, a Narishige IM300 microinjector, and a Leitz DMIL microscope (HMC 40/0.5 objective, Leica). Protein solutions (0.5–1.0 mg/ml) in buffer A were centrifuged at 20,800 × g at 4 °C for 15 min prior to injection. Cells were plated on 4-cm round coverslips in 10-cm dishes and were cultured for 12–48 h. Cells were injected with protein, and the coverslips were returned to the incubator for 20 min to 2 h. Coverslips were subsequently installed in a heated perfusion chamber (Focht Live-Cell chamber System FCS2, Bioptechs), and cells were examined using a Bio-Rad MRC 600 confocal laser scanning microscope with a heated 60/1.40 oil immersion lens (Nikon) at 37 °C (lens heater from Bioptechs). Cells transfected with EGFP-C2 or microinjected with C2-cPLA$_2$-Alexa were observed with and without the calcium ionophore A23187 (10 μM), and the medium was supplemented with $CaCl_2$ (200 μM). Cells transiently transfected with pEGFP-tK and pEGFP-K-Ras were examined using medium containing 3 μM paclitaxel or Me_2SO vehicle. Examination of paclitaxel cells microinjected with sgGFP-D-tK was carried out by first treating the cells with paclitaxel for 2 h at 37 °C, followed by microinjection, further incubation with paclitaxel for 3 h, and subsequent confocal analysis.

RESULTS

Preparation of sgGFP-K-Ras4B Conjugates—The structures of the fluorescent electrostatic probes sgGFP-L-tK and sgGFP-D-tK are shown in Fig. 2. The probe consists of the last 12 residues of K-Ras4B (32) cross-linked to a GFP variant. An *N*-acetylcysteine was placed at the N terminus to allow linking to GFP. The two cysteine residues were orthogonally protected, allowing individual modification. After side-chain deprotection, the C-terminal cysteine was selectively farnesylated using a regioselective method (27). The N-terminal cysteine disulfide was reduced and reacted with an excess of bis-iodoacetamide linker. sgGFP, a GFP suitable for bacterial expression with a single enhanced excitation peak, was chosen as the fluorophore. sgGFP did not contain any cysteines sufficiently solvent-exposed for conjugation as assessed by Ellman assay (33). Therefore a new cysteine residue was introduced at the C terminus of the protein by mutagenesis.

sgGFP N239C was stored in reducing buffer to prevent its facile conversion to the disulfide dimer (assessed by SDS-PAGE). Following reducing agent removal, the conjugation reaction was conducted at 0 °C in pH 8.0 buffer containing a protease inhibitor mixture and an excess of the peptide-linker. The most successful results were obtained when 4 eq of the peptide-linker were added portion-wise over 2 h, with storage at −20 °C prior to purification. The optimum conditions for the conjugation reaction were established after multiple failed attempts, which led to various proteolyzed products. It has been observed that the C-terminal 7–9 residues of wild type GFP are readily removed upon incubation with trypsin or Pronase (34). Introduction of an additional 13-amino acid sequence at this position might increase any inherent flexibility in the C-terminal region, and residual protease activity in the sample from bacterial expression acts on either the *all*-L peptide-linker region or the C-terminal sgGFP N239C region of sgGFP-L-tK. After extended periods of time, samples of sgGFP exhibited MALDI mass spectra ~700–800 Da less than the expected mass, corresponding to the loss of 6–7 amino acids from the C terminus. Conjugation samples kept at room temperature displayed masses from 300–900 Da less than the expected mass, which corresponds to the loss of 1–6 of the C-terminal amino acids in the K-Ras4B peptide. This phenomenon was more pronounced in the case of the *all*-L peptide conjugate, understandably, because the *all*-D peptide sequence would be expected to be protease resistant. The optimized conditions afforded samples that, after purification, had 80–90% purity when assessed by visual examination of SDS-PAGE gels. The mass of the conjugates determined by MALDI mass spectrom-

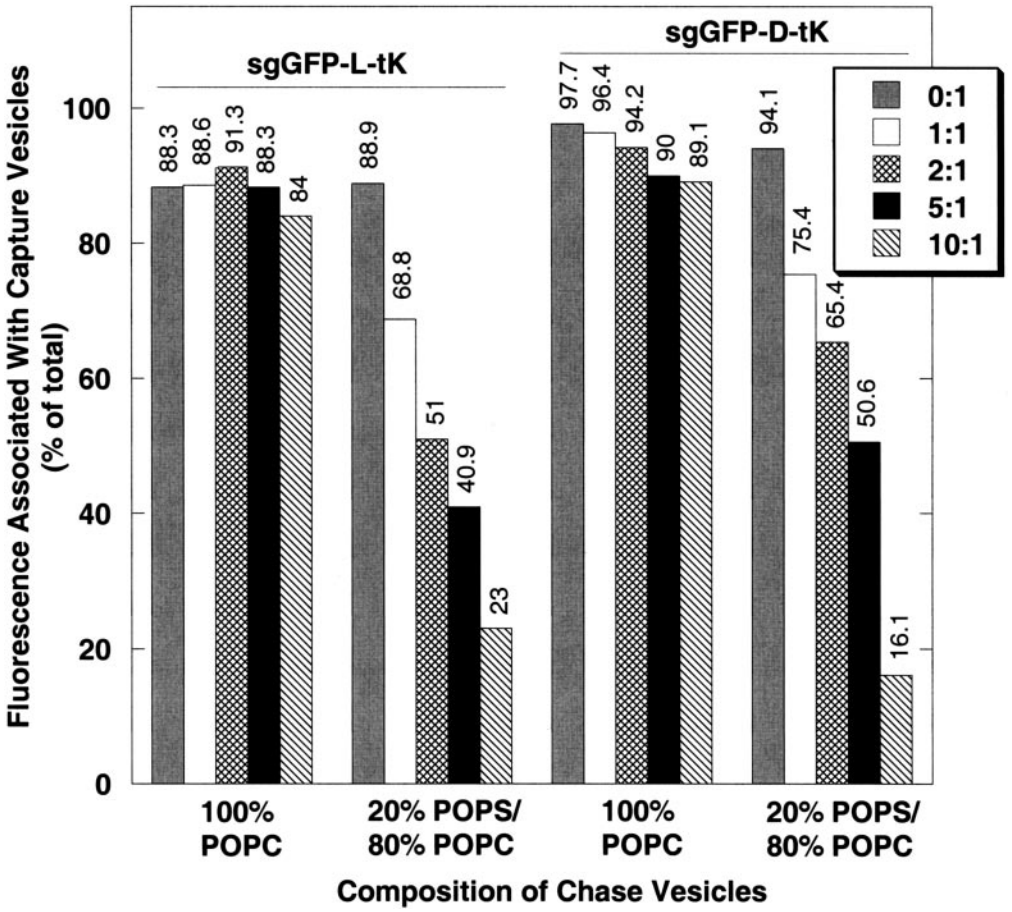

FIG. 1. **Competitive binding of sgGFP-L-tK (*left two clusters*) and sgGFP-D-tK (*right two clusters*) conjugates to phospholipid vesicles.** Protein conjugates were added to anionic capture vesicles (20% POPS/80% POPC) followed by the addition of either purely zwitterionic chase vesicles (100% POPC) or anionic chase vesicles (20% POPS/80% POPC) as indicated along the *x*-axis. Capture vesicles were loaded with sucrose, chase vesicles were loaded with KCl, and the different vesicles were separated by ultracentrifugation. The *y*-axis gives the percent of total protein conjugate fluorescence that is recovered in the bottom half of the centrifuge tube (bound to capture vesicles). The *inset* gives the ratio of chase to capture vesicles.

etry was within 0.5% of the calculated values.

Vesicle Binding Properties—We anticipated that the conjugates sgGFP-L-tK and sgGFP-D-tK would bind to acidic phospholipids in preference to zwitterionic phospholipids and that both conjugates would behave similarly, even though the phospholipids are chiral. Studies with the N terminus of SRC (14) have indicated that the myristate group penetrates into the hydrocarbon interior of the membrane while the polar N-terminal glycine residue remains in the aqueous phase, immediately outside the envelope of the polar head group region. The basic lipopeptide adopts a random coil configuration and lies on the membrane surface. Thus the basic amino acids are not likely to directly contact the chiral glycerol backbone, lending credence to the prediction that the *all*-L and *all*-D peptides should show similar binding preferences.

To determine the relative binding of each conjugate to 100% POPC vesicles *versus* vesicles composed of 20% POPS/80% POPC, a fluorometric competition binding assay was developed using sucrose-loaded POPS/POPC vesicles and KCl-loaded POPC vesicles with a glucose-containing centrifugation buffer. The external glucose-containing buffer has an intermediate density to those of the buffers trapped within the POPC and POPS/POPC vesicles, guaranteeing that the vesicles will be separable via ultracentrifugation. Sucrose-loaded POPS/POPC vesicles were doped with a trace amount of ^{3}H-labeled phospholipid, whereas POPC vesicles contained a trace amount of ^{14}C-labeled phospholipid so that the different types of vesicles could be tracked following centrifugation. Initial studies demonstrated that at high concentrations of 20% POPS/80% POPC vesicles (total phospholipid concentration > 2 mM), ~80% of the fluorescence of sgGFP-D-tK or sgGFP-L-tK samples was bound to the vesicles (not shown). We attributed the fluorescence in the supernatant to small amounts of sgGFP lacking the K-Ras4B peptide either due to incomplete conjugation of peptide to protein or to proteolytic cleavage of the C terminus during sample handling. Thus, after an initial centrifugation step to pellet sucrose-loaded POPS/POPC vesicles, the supernatant was discarded, and the pellet was resuspended in buffer containing various amounts of KCl-loaded POPC vesicles. Following a second ultracentrifugation step, the sample tubes were immediately frozen and cut to ensure efficient separation of the floating POPC and pelleted POPS/POPC vesicles. The amount of fluorescent conjugate present in the upper half, containing ≥80% of the POPC vesicles, and the amount present in the lower half, with ≥95% of the POPS/POPC vesicles, was analyzed by fluorometry.

Binding data for the sgGFP-L-tK and sgGFP-D-tK conjugates with POPC and POPS/POPC vesicles is presented in Fig. 1. For both conjugates, the equilibrium constant for the binding of the conjugate to 20% POPS/80% POPC vesicles is at least 10 times that for the binding to pure POPC vesicles, because a 10-fold excess of pure POPC vesicles failed to extract even 50% of the peptide-protein conjugates from the POPS/POPC vesicles.

To examine if the initial binding of the conjugates to the sucrose-loaded POPS/POPC vesicles is reversible, the same experiment was performed using KCl-loaded POPS/POPC

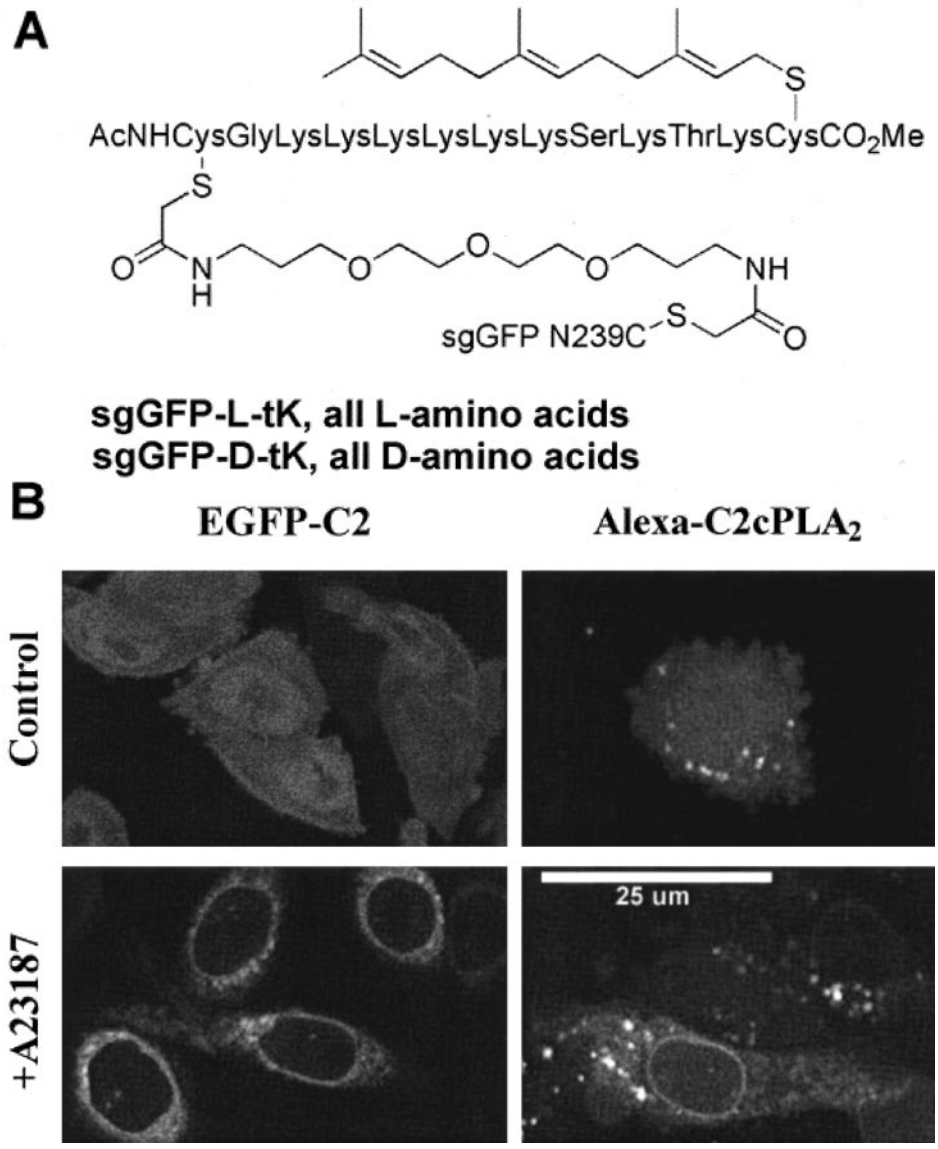

FIG. 2. *A*, sgGFP-L-tK and sgGFP-D-tK. *B*, comparison of the effect of Ca^{2+} ionophore on targeting of C2-cPLA$_2$. Confocal images of CHO cells transfected with pEGFP-C2-cPLA$_2$ (*left panels*) and MDCK cells microinjected with Alexa-C2-cPLA$_2$ (*right panels*). Cells were examined with (*lower panels*) and without (*upper panels*) Ca^{2+} ionophore A23187. Microinjection into CHO cells showed similar results (not shown). The *scale bar* represents the scale for all four panels. The *lower right panel* shows more than one cell, the central cell, and others surrounding it but with much lower fluorescence due to variation in the amount of protein microinjected.

chase vesicles. Binding data for this experiment is also presented in Fig. 1. For both conjugates the fluorescence is extracted from the sucrose-loaded POPS/POPC vesicles in a manner dependent on POPS/POPC chase vesicle concentration. With a 10-fold excess of POPS/POPC chase vesicle, most of the fluorescent protein, ~80%, is extracted from the vesicle pellet. The small amount of fluorescence in the pellet, ~20%, can be explained by the fact that centrifugation of the protein without any vesicles also results in an enrichment of fluorescence in the pellet fraction of about 20%, suggesting that some of the conjugate aggregates and sediments during centrifugation. This binding required the K-Ras4B peptide, because <16% of unconjugated sgGFP N239C binds to either POPC or POPS/POPC sucrose-loaded vesicles (not shown). These results establish that both sgGFP-L-tK and sgGFP-D-tK conjugates show a dramatic preference for binding to anionic vesicles *versus* zwitterionic vesicles and that their binding to 20% POPS/POPC vesicles is reversible.

Cell Culture Studies—We studied two proteins that are known to target to different intracellular membranes. Previous work has shown that cPLA$_2$ translocates from the cytosol to the perinuclear membranes of mammalian cells in response to an increase in intracellular calcium (8, 9). On the other hand K-Ras4B is found mainly on the cytosolic face of the plasma membrane (12, 13). CHO cells were stably transfected with a plasmid encoding EGFP fused to the C2 domain of cPLA$_2$. The distribution of EGFP-C2cPLA$_2$ was examined in living cells at 37 °C by confocal fluorescence microscopy. As shown in Fig. 2, EGFP-C2cPLA$_2$ was detected throughout the cell and was recruited to and concentrated at the perinuclear region upon addition of Ca^{2+} and Ca^{2+} ionophore to the medium, specifically observed as brighter fluorescence surrounding the nucleus of the cell and at the Golgi and ER (Fig. 2*B*, *lower left panel*).

To validate the microinjection approach, we tagged the recombinant C2-cPLA$_2$ protein with a fluorescent marker and microinjected it into live cells. The protein was indeed recruited to the perinuclear region of either CHO or MDCK cells upon addition of Ca^{2+} and Ca^{2+} ionophore to the medium (Fig. 2), also specifically observed as a defined band surrounding the nucleus of the cell (Fig. 2*B*, *lower right panel*). Some punctate fluorescence is observed in both the ionophore-treated and untreated cells; however, the amount of this fluorescence varies from cell to cell and is probably dependent on the amount of Alexa-C2cPLA$_2$ that actually enters the cell. The amount of protein that enters the cell differs for each injection due to changes in the pressure if the needle becomes partially blocked with cellular debris, the length of time the injection is allowed

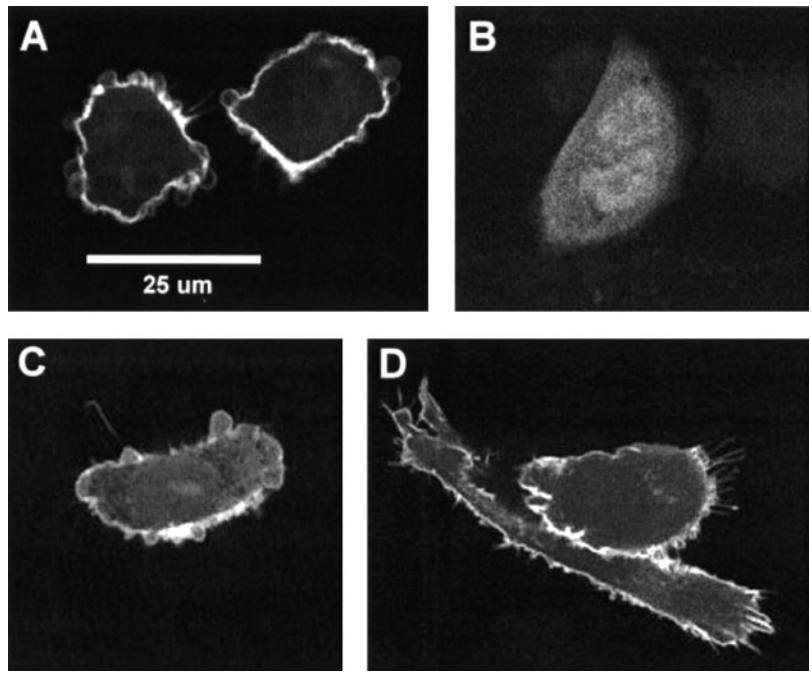

FIG. 3. **Confocal images of CHO cells transfected with pEGFP-tK (*A*), injected with sgGFP N239C (*B*), injected with sgGFP-L-tK (*C*), injected with sgGFP-D-tK (*D*).** The *scale bar* represents the scale for all four panels.

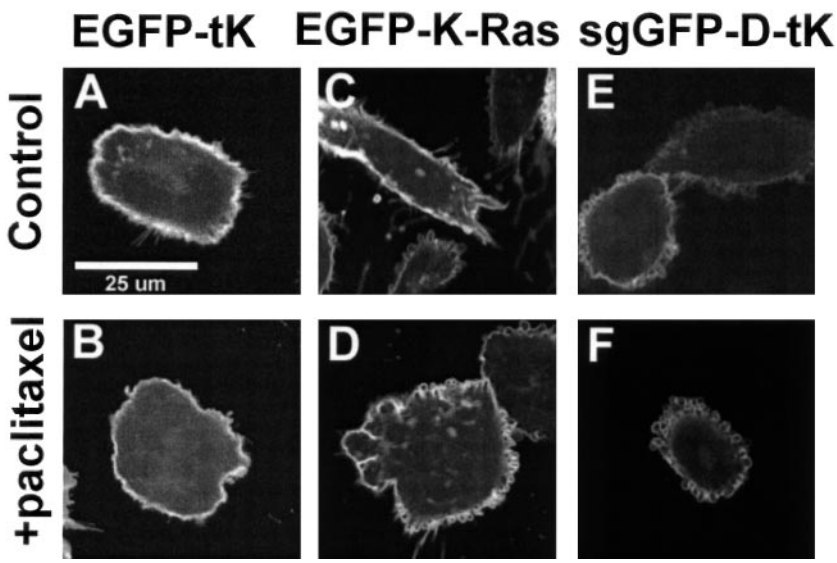

FIG. 4. **Confocal images of CHO cells transfected with pEGFP-tK (*A* and *B*), transfected with EGFP-K-Ras (*C* and *D*), and injected with sgGFP-D-tK (*E* and *F*).** Cells were treated with vehicle (Me_2SO, *top panels*) or 3 μM paclitaxel (*bottom panels*). The *scale bar* represents the scale for all six panels. Variation in fluorescence intensity in *panels E* and *F* arise from variation in the amount of protein microinjected.

to proceed, and the efficiency of puncturing the cell membrane. The C2 domain may be aggregating either before or after injection, which could produce the punctate fluorescence observed. Such staining was not observed with the protein conjugates and so probably arises from some property of the C2 domain itself. Nevertheless, the obvious targeting of the nuclear envelope illustrates that the microinjected protein targeted the same intracellular membranes in response to a rise in intracellular Ca^{2+} as did the EGFP-C2cPLA$_2$ fusion protein produced by transfection. This demonstrates that proteins that target the intracellular membranes can indeed be visualized on these membranes after microinjection.

As shown in Fig. 3*A*, when CHO cells were transfected with the plasmid pEGFP-tK that produces EGFP with the C-terminal 17 amino acids of K-Ras4B (30) (hereafter designated EGFP-tK), virtually all of the fluorescence in living cells was from the plasma membrane as has been observed with this chimera expressed in other cell types (30). When CHO or MDCK cells were microinjected with sgGFP-L-tK, the same plasma membrane localization was seen as for EGFP-tK (Fig. 3*C*). CHO and MDCK cells microinjected with the fluorescent protein lacking the K-Ras4B C terminus, sgGFP N239C, showed diffuse fluorescence throughout the cytoplasm and nucleus (Fig. 3*B*). Thus, the K-Ras4B C-terminal peptide is required for plasma membrane localization of sgGFP-L-tK. Finally, when CHO and MDCK cells were microinjected with the green fluorescent protein bearing the K-Ras4B C terminus composed of all-D-amino acids, sgGFP-D-tK, virtually all of the fluorescent signal was from the plasma membrane (Fig. 3*D*).

The effect of paclitaxel-mediated disruption of the microtubule network on the localization of EGFP-tK and EGFP-K-Ras was examined in CHO cells by transfection with pEGFP-tK or pEGFP-K-Ras into cells pre-treated with paclitaxel. After 24 h, confocal microscopy revealed that, although the paclitaxel-treated CHO cells showed obvious effects of the drug, including arrested growth and the loss of elongated shape often associated with disruption of the intact microtubule network in fibroblasts and polarized cells (35–37), the full-length and truncated K-Ras4B fusions nevertheless accumulated at the plasma membrane (Fig. 4, *A–D*). This result is in contrast to the report

by Casey and coworkers in which paclitaxel treatment of NIH3T3 cells prior to transfection with a plasmid encoding a GFP fusion to the full-length K-Ras4B protein resulted in disrupted K-Ras4B targeting (22, 23). The K-Ras4B conjugate sgGFP-D-tK also exhibited retention of plasma membrane targeting in paclitaxel-treated CHO cells (Fig. 4, *E* and *F*). It should be kept in mind that slight variations in the intensity of fluorescence observed in the microinjected cells arise from differences in the amount of conjugate actually entering each cell. Fig. 4*E* shows two cells with different fluorescence intensities despite the fact that both were grown and analyzed under the same conditions on the same coverslip. These results strongly suggest that microtubule shuttling is not required for targeting of these K-Ras4B constructs to the plasma membrane.

DISCUSSION

The plasma membrane localization of the K-ras4B protein has been previously determined to be directed by its post-translationally modified C-terminal sequence (12, 18, 38), which can also act as an independent plasma-membrane targeting signal when coupled to heterologous proteins (22, 30, 39–41). Although the necessary signal for K-Ras4B localization has been well established, the mechanism by which it is directed to and maintained at the plasma membrane after post-translational modification is still largely undefined. Clarification of these concerns may be of broader interest due to the existence of lipidated/polybasic motifs in other intracellular proteins (14–16, 42). Various suggestions have been made to explain K-Ras4B trafficking, including the potential existence of a membrane receptor (21), the proposed interaction of the polybasic domain with the phospholipid membrane (13, 14), and the possible involvement of microtubules in the directing process (22). It is difficult to determine which of these mechanisms is operative, especially because the asymmetric distribution of phospholipids across the internal membranes of mammalian cells is currently obscure. Therefore we chose to develop an electrostatic membrane probe based on the C-terminal sequence of K-Ras4B to address this issue. To permit direct visualization of targeting mediated by the K-Ras4B C-terminal sequence in living cells, we conjugated it to a fluorescent tag. The ubiquitous use of GFP as a fluorescent tag in biological systems, and even for imaging of K-Ras fusions (22, 30, 43), made it an ideal choice. Additionally, it has been shown that GFP diffuses freely in mammalian cells, and the large size of GFP prevents nuclear localization of the small polybasic peptides (44).

It was important to establish that both the *all*-L and *all*-D peptide conjugates display similar preference for binding to acidic PS-containing PC membranes over those that lack the anionic phospholipid. In this way, the binding behavior of the *all*-D conjugate can be directly correlated to electrostatic effects and can be expected to be nearly identical to the behavior of the *all*-L conjugate in the absence of a K-Ras4B receptor protein in cells. The ability of each conjugate to bind to LUVs *in vitro* was examined with a vesicle-binding competition assay. The results demonstrate that the *all*-D peptide conjugate displays the same preferential binging to PS-containing PC vesicles over pure PC vesicles as the *all*-L peptide conjugate.

Control microinjection experiments with the C2 domain of $cPLA_2$ importantly show that the localization is not affected by any artifacts of the microinjection procedure. The results obtained were essentially identical to the results observed with cells transfected with EGFP-C2cPLA_2. Our findings using the sgGFP N239C conjugates support the model in which the plasma membrane-targeting function of the K-Ras4B C-terminal region depends on the electrostatic attraction between the polybasic peptide and acidic phospholipids. The plasma membrane staining of cells injected with both the *all*-L and *all*-D peptide conjugates suggests that this targeting signal is accomplished by a non-receptor, membrane electrostatic mechanism, however it must be noted that it does not exclude the possibility that a putative membrane-bound protein receptor exists that has a very low specificity of binding. Such a binding site would need to be able to accommodate not only the *all*-L amino acid sequence but also the D-amino acid sequence and a sequence in which the lysine residues have been mutated to arginine residues, because this mutant of the K-Ras4B protein has also been shown to possess the full activity of the wild type sequence (12). Such features of a putative protein receptor seem highly unlikely. However, mutation of the lysine residues to glutamine results in loss of the targeting function. These results suggest that the binding is not dependent on the geometry of the peptide but on the charge of the sequence.

Additional support for the role of charge in targeting is provided by nuclear lamin B3b, which possess a C*AAX* motif, a polybasic region, a nuclear localization signal (NLS), and is targeted to the inner nuclear membrane. Disruption of the NLS results in plasma membrane localization (45). There is presumably no natural receptor for this lamin in the plasma membrane, because lamins are targeted to the nucleus and the modified sequence lacking the NLS is non-natural, suggesting that the resulting plasma membrane localization of the polybasic farnesylated sequence is guided by a nonspecific interaction similar to the K-Ras4B protein.

We additionally addressed the question of microtubule-directed K-Ras4B targeting by observing K-Ras4B GFP conjugates in living cells in the presence of paclitaxel, a microtubule stabilizing agent. Our findings with CHO cells show that targeting of the full-length or truncated K-Ras4B protein is unaffected by incubation with paclitaxel. Additionally, we microinjected paclitaxel-treated cells with sgGFP-D-tK and observed plasma membrane staining. These results suggest that, in CHO cells, perturbation of the microtubule network does not affect proper targeting of K-Ras4B or our fluorescent probes, a conclusion that is at odds with the results of Casey and coworkers in NIH3T3 cells (22, 23). Our results suggest that the amount of anionic phospholipid in the cytosol-facing internal membranes is less than in the cytosol-facing leaflet of the plasma membrane, because both cationic probes accumulate on the latter; however, the data does not imply that the cytosol-facing internal membranes lack any anionic phospholipids.

With this in mind, electrostatic attraction or repulsion of residues residing at the binding sites of peripheral membrane proteins could play an integral role in the membrane binding, or enhancement of the binding, of these proteins. Notably, the calcium-dependent binding of the C2 domain of $cPLA_2$, shown to exhibit a preference for zwitterionic PC vesicles over the anionic PS vesicles (10, 46), is directed to the perinuclear region. It has been proposed that the binding interactions of C2-$cPLA_2$ are predominantly hydrophobic and that calcium enhances C2-$cPLA_2$ binding to PC vesicles by acting as an electrostatic switch to neutralize the anionic carboxylate ligands coming from the protein, assisting in insertion of the hydrophobic surface loop of the protein into the core of the membrane (31, 47–52). The observation that the cytosolic faces of the internal membranes possess a lower proportion of acidic phospholipids supports this rationalization of C2-$cPLA_2$ membrane binding.

Acknowledgments—We are grateful to F. Ghomashchi for preparation of C2-$cPLA_2$-Alexa, and J. Hancock and C. Leslie for providing EGFP fusion protein plasmids.

REFERENCES

1. Bruckheimer, E. M., and Schroit, A. J. (1996) *J. Leukoc. Biol.* **59,** 784–788
2. Devaux, P. F. (1991) *Biochemistry* **30,** 1163–1173
3. Etemadi, A. H. (1980) *Biochim. Biophys. Acta* **604,** 423–475
4. Bevers, E. M., Comfurius, P., Dekkers, D. W., and Zwaal, R. F. (1999) *Biochim. Biophys. Acta* **1439,** 317–330
5. Diaz, C., and Schroit, A. J. (1996) *J. Membr. Biol.* **151,** 1–9
6. Higgins, C. F. (1994) *Cell* **79,** 393–395
7. Pomorski, T., Hrafnsdottir, S., Devaux, P. F., and van Meer, G. (2001) *Semin. Cell Dev. Biol.* **12,** 139–148
8. Glover, S., de Carvalho, M. S., Bayburt, T., Jonas, M., Chi, E., Leslie, C. C., and Gelb, M. H. (1995) *J. Biol. Chem.* **270,** 15359–15367
9. Schievella, A. R., Regier, M. K., Smith, W. L., and Lin, L. L. (1995) *J. Biol. Chem.* **270,** 30749–30754
10. Nalefski, E. A., McDonagh, T., Somers, W., Seehra, J., Falke, J. J., and Clark, J. D. (1998) *J. Biol. Chem.* **273,** 1365–1372
11. Mosior, M., Six, D. A., and Dennis, E. A. (1998) *J. Biol. Chem.* **273,** 2184–2191
12. Hancock, J. F., Cadwallader, K., Paterson, H., and Marshall, C. J. (1991) *EMBO J.* **10,** 4033–4039
13. Ghomashchi, F., Zhang, X., Liu, L., and Gelb, M. H. (1995) *Biochemistry* **34,** 11910–11918
14. Buser, C. A., Sigal, C. T., Resh, M. D., and McLaughlin, S. (1994) *Biochemistry* **33,** 13093–13101
15. Murray, D., Ben-Tal, N., Honig, B., and McLaughlin, S. (1997) *Structure* **5,** 985–989
16. Resh, M. D. (1994) *Cell* **76,** 411–413
17. Leventis, R., and Silvius, J. R. (1998) *Biochemistry* **37,** 7640–7648
18. Hancock, J. F., Paterson, H., and Marshall, C. J. (1990) *Cell* **63,** 133–139
19. McLaughlin, S., and Aderem, A. (1995) *Trends Biochem. Sci.* **20,** 272–276
20. Sigal, C. T., Zhou, W., Buser, C. A., McLaughlin, S., and Resh, M. D. (1994) *Proc. Natl. Acad. Sci. U. S. A.* **91,** 12253–12257
21. Jansen, B., Schlagbauer-Wadl, H., Kahr, H., Heere-Ress, E., Mayer, B. X., Eichler, H., Pehamberger, H., Gana-Weisz, M., Ben-David, E., Kloog, Y., and Wolff, K. (1999) *Proc. Natl. Acad. Sci. U. S. A.* **96,** 14019–14024
22. Chen, Z., Otto, J. C., Bergo, M. O., Young, S. G., and Casey, P. J. (2000) *J. Biol. Chem.* **275,** 41251–41257
23. Thissen, J. A., Gross, J. M., Subramanian, K., Meyer, T., and Casey, P. J. (1997) *J. Biol. Chem.* **272,** 30362–30370
24. Thissen, J. A., and Casey, P. J. (1993) *J. Biol. Chem.* **268,** 13780–13783
25. Resh, M. D. (1989) *Cell* **58,** 281–286
26. Nakatani, Y., Tanioka, T., Sunaga, S., Murakami, M., and Kudo, I. (2000) *J. Biol. Chem.* **275,** 1161–1168
27. Xue, C. B., Becker, J. M., and Naider, F. (1992) *Tetrahedron Lett.* **33,** 1435–1438
28. Yakhnin, A. V., Vinokurov, L. M., Surin, A. K., and Alakhov, Y. B. (1998) *Protein Expr. Purif.* **14,** 382–386
29. Johnson, B. H., and Hecht, M. H. (1994) *Biotechnology* **12,** 1357–1360
30. Apolloni, A., Prior, I. A., Lindsay, M., Parton, R. G., and Hancock, J. F. (2000) *Mol. Cell. Biol.* **20,** 2475–2487
31. Ball, A., Nielsen, R., Gelb, M. H., and Robinson, B. H. (1999) *Proc. Natl. Acad. Sci. U. S. A.* **96,** 6637–6642
32. McGrath, J. P., Capon, D. J., Smith, D. H., Chen, E. Y., Seeburg, P. H., Goeddel, D. V., and Levinson, A. D. (1983) *Nature* **304,** 501–506
33. Ellman, G. L. (1959) *Arch. Biochem. Biophys.* **82,** 70–77
34. Chiang, C. F., Okou, D. T., Griffin, T. B., Verret, C. R., and Williams, M. N. (2001) *Arch. Biochem. Biophys.* **394,** 229–235
35. Schiff, P. B., and Horwitz, S. B. (1980) *Proc. Natl. Acad. Sci. U. S. A.* **77,** 1561–1565
36. Gloushankova, N. A., Lyubimova, A. V., Tint, I. S., Feder, H. H., Vasiliev, J. M., and Gelfand, I. M. (1994) *Proc. Natl. Acad. Sci. U. S. A.* **91,** 8597–8601
37. Pletjushkina, O. J., Ivanova, O. J., Kaverina, I. N., and Vasiliev, J. M. (1994) *Exp. Cell Res.* **212,** 201–208
38. Jackson, J. H., Li, J. W., Buss, J. E., Der, C. J., and Cochrane, C. G. (1994) *Proc. Natl. Acad. Sci. U. S. A.* **91,** 12730–12734
39. Huang, D. C., Marshall, C. J., and Hancock, J. F. (1993) *Mol. Cell. Biol.* **13,** 2420–2431
40. Stokoe, D., Macdonald, S. G., Cadwallader, K., Symons, M., and Hancock, J. F. (1994) *Science* **264,** 1463–1467
41. Leevers, S. J., Paterson, H. F., and Marshall, C. J. (1994) *Nature* **369,** 411–414
42. Beranger, F., Goud, B., Tavitian, A., and de Gunzburg, J. (1991) *Proc. Natl. Acad. Sci. U. S. A.* **88,** 1606–1610
43. Yokoe, H., and Meyer, T. (1996) *Nat. Biotechnol.* **14,** 1252–1256
44. Christophe, D., Christophe-Hobertus, C., and Pichon, B. (2000) *Cell. Signalling* **12,** 337–341
45. Hofemeister, H., Weber, K., and Stick, R. (2000) *Mol. Biol. Cell* **11,** 3233–3246
46. Hixon, M. S., Ball, A., and Gelb, M. H. (1998) *Biochemistry* **37,** 8516–8526
47. Davletov, B., Perisic, O., and Williams, R. L. (1998) *J. Biol. Chem.* **273,** 19093–19096
48. Perisic, O., Fong, S., Lynch, D. E., Bycroft, M., and Williams, R. L. (1998) *J. Biol. Chem.* **273,** 1596–1604
49. Gerber, S. H., Rizo, J., and Sudhof, T. C. (2001) *J. Biol. Chem.* **276,** 32288–32292
50. Xu, G. Y., McDonagh, T., Yu, H. A., Nalefski, E. A., Clark, J. D., and Cumming, D. A. (1998) *J. Mol. Biol.* **280,** 485–500
51. Bittova, L., Sumandea, M., and Cho, W. (1999) *J. Biol. Chem.* **274,** 9665–9672
52. Nalefski, E. A., and Newton, A. C. (2001) *Biochemistry* **40,** 13216–13229